COMSOL
CONFERENCE
2024 FLORENCE

Atmospheric Plasma Modelling Applied For Thermal Plasma Assisted Processes

A. Lejeune[1]
1. R&D and Simulation, PROTOSTEP, Cergy-Pontoise, France.

Abstract
The current general context for green production and decarbonation prompts considering alternative solutions to produce high added value byproducts from gas decomposition without producing CO2. Steam Reforming or Combustion processes, widely applied in Industry, need H2O or O2 to activate the gas decomposition, originating in CO2 formation in the presence of Hydrocarbon elements. An alternative solution to decompose Hydrocarbon elements without CO2 formation is to activate the decomposition in a high temperature plasma. In that way, there is no need of H2O or O2 to activate the gas decomposition since the plasma is ignited and heated from electron collisions - thermodynamic equilibrium is still governed by neutrals, but electromagnetic energy transfer is governed by electrons. Atmospheric plasmas, also called Thermal plasmas, are much more challenging to be simulated than at low pressure since high gas temperature and skin effect are expected from thermodynamic and electromagnetic coupling. Thermal plasmas used in industry have a low degree of ionization and thus MHD can be neglected. In this paper, we will present the results obtained with COMSOL Multiphysics® in a 915MHz microwave Argon plasma. Plasma module is used to compute electron density and temperature under microwave exposure. CFD module is used to compute gas flow and coupling with thermal properties. Heat transfer module is used to compute the gas temperature rise according to the thermodynamic properties. RF module is used to simulate the wave propagation at 915MHz and the plasma to waveguide coupling. The presented model combines the physics observed separately in the models from the Application Libraries: In-Plane Microwave Plasma (Application ID: 8664), Inductively Coupled Plasma (ICP) Torch (Application ID: 18125), Thermal Plasma (Application ID: 8658) and Coaxial to Waveguide Coupling (Application ID: 1863). The plasma properties and electromagnetic coupling will be compared at low and atmospheric pressure ranges. We will discuss the main differences observed in a glow discharge and a thermal plasma.

Keywords: Argon, Microwave, Thermal plasma, Electron collisions, Thermodynamic equilibrium, Coaxial to waveguide coupling, Skin effect.

Introduction
Microwave plasmas (0.3-300GHz) are used in industry for various applications such as in microelectronics or decomposition of greenhouse gases [1]. Contrary to the use of DC plasmas, microwave plasmas do not need electrodes that may pollute or disturb the discharge at high pressure. Furthermore, contrary to the evanescent mode occurring in the RF plasmas at lower frequency (13.56MHz, 27.12MHz), the microwave frequency (915MHz, 2450MHz) can be propagative [2]. High pressure microwave plasmas are still studied in laboratories since they are experimentally characterized by specific phenomena of contraction or filamentation under given conditions that may affect the stability of the discharge and thus be a limitation for an industrial application [1]. In that context, the modelling of a microwave plasma with COMSOL Multiphysics® is a necessary step to optimize the development of a plasma reactor for a given application.

Experimental Set Up
The system presented in this paper (Fig.1) is a 915MHz microwave plasma source operating with an Argon gas flow at atmospheric pressure. A 10kW magnetron is used as a microwave source and a standard rectangular waveguide WR975 propagates the microwave up to a Quartz cylinder inserted in a cylindrical cavity. The Quartz cylinder is fed with a continuous gas flow from which the plasma is created. A movable plunger allows to center the maximum electric field in the Quartz tube. Formation of plasma is usually governed by a reaction set including the electron collisions depending on the electron temperature T_e in eV and the thermochemical reactions depending on the gas temperature T in K[1]. Contrary to what it is observed in the fusion plasmas with a high degree of ionization (~ 1) and high gas temperature ($\sim 10^6$K) , the degree of ionization in the thermal plasmas as used in laboratory or industry remains low ($\ll 10^{-3}$) with a gas temperature in the range of a few 10^3K at local thermodynamic equilibrium ($T_e \sim T$). However, this

[1] 1eV=11600K

property is sufficient to operate the thermochemistry processes as used in thermal gas decomposition. In the present paper, we will only consider the electron collision processes in Argon (Ar) to ignite an Ar plasma with creation of Ar ions and the first excited states including their physical properties.

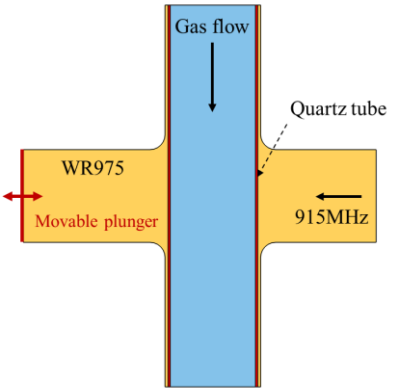

Figure 1. Experimental set-up.

Theory

Microwave propagation in a waveguide

The electromagnetic fields propagate in a waveguide according to the Maxwell's equations [3]:

$$\begin{aligned} \nabla \times \boldsymbol{E} &= -\frac{\partial \boldsymbol{B}}{\partial t} \quad \nabla . \boldsymbol{E} = 0 \\ \nabla \times \boldsymbol{B} &= \mu\varepsilon \frac{\partial \boldsymbol{E}}{\partial t} \quad \nabla . \boldsymbol{B} = 0 \end{aligned} \tag{1}$$

and the boundary conditions at the walls:

$$\begin{aligned} \mathbf{n} \times \boldsymbol{E} &= 0 \\ \mathbf{n} . \boldsymbol{B} &= 0 \end{aligned} \tag{2}$$

In a rectangular waveguide of dimensions (a, b):

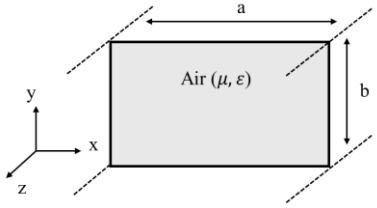

Figure 2. Cross-section of the rectangular waveguide.

with a wave propagation along the z-direction at frequency $\omega = 2\pi f$:

$$\begin{cases} \boldsymbol{E}(\boldsymbol{r},t) = \boldsymbol{E}(x,y)e^{-i\omega t}e^{ikz} \\ \boldsymbol{B}(\boldsymbol{r},t) = \boldsymbol{B}(x,y)e^{-i\omega t}e^{ikz} \end{cases} \tag{3}$$

the relationship for the wavenumber is given by:

$${k_{mn}}^2 = \mu\varepsilon\omega^2 - \pi^2\left(\frac{m^2}{a^2} + \frac{n^2}{b^2}\right) > 0 \tag{4}$$

The wave propagates only if the wavenumber is real and positive, so with a microwave frequency ω above the cutoff frequency ω_{mn}:

$$\omega > \omega_{mn} = \frac{\pi}{\sqrt{\mu\varepsilon}}\left(\frac{m^2}{a^2} + \frac{n^2}{b^2}\right)^{\frac{1}{2}} \tag{5}$$

By considering a frequency $f = 915\text{MHz}$ in a standard waveguide WR975, we identify the mode ω_{10} as the dominant propagative mode. It corresponds to the transverse electric TE_{10} mode:

$$\boldsymbol{E}(\boldsymbol{r},t) = \begin{cases} E_x = 0 \\ E_y = i\omega B_0 \left(\frac{a}{\pi}\right) \sin\left(\frac{\pi x}{a}\right) e^{-i\omega t}e^{ikz} \\ E_z = 0 \end{cases} \tag{6}$$

with:

$$\begin{aligned} k^2 = {k_{10}}^2 &= \mu\varepsilon\omega^2 - \frac{\pi^2}{a^2} \\ 0 \le x &\le a \end{aligned} \tag{7}$$

Microwave propagation in a plasma

Inside a plasma (μ_r, ε_r) containing charged particles, the wave propagation is driven by:

$$\begin{aligned} \nabla \times \boldsymbol{E} &= -\frac{\partial \boldsymbol{B}}{\partial t} \qquad \nabla . \boldsymbol{E} = \frac{\rho}{\varepsilon_0 \varepsilon_r} \\ \nabla \times \boldsymbol{B} &= \mu_0\mu_r \boldsymbol{j} + \frac{\mu_r\varepsilon_r}{c^2}\frac{\partial \boldsymbol{E}}{\partial t} \qquad \nabla . \boldsymbol{B} = 0 \end{aligned} \tag{10}$$

A general solution is expressed with k having a complex form:

$$\begin{aligned} \boldsymbol{E}(\boldsymbol{r},t) &= \boldsymbol{E}(x,y)e^{-i\omega t}e^{ikz} \\ k &= a + ib \end{aligned} \tag{11}$$

When $b \neq 0$, the plasma is dispersive with a dispersion relation defined by:

$$k^2 = \frac{\omega^2}{c^2}\varepsilon_r(\omega) \tag{12}$$

and:

$$\varepsilon_r(\omega) = 1 - \frac{\omega_p^2}{\omega^2 + \nu_m^2} - i\frac{\nu_m}{\omega}\left(\frac{\omega_p^2}{\omega^2 + \nu_m^2}\right) \tag{13}$$

where ω_p is the plasma frequency:

$$\omega_p = \left(\frac{n_e e^2}{m_e \varepsilon_0}\right)^{\frac{1}{2}} \tag{14}$$

At high frequency (ω) and low collision frequency (ν_m), the dispersion relation in the plasma becomes:

$$\begin{aligned} \omega^2 &= {\omega_p}^2 + k^2c^2 \\ \nu_m &\ll \omega \end{aligned} \tag{15}$$

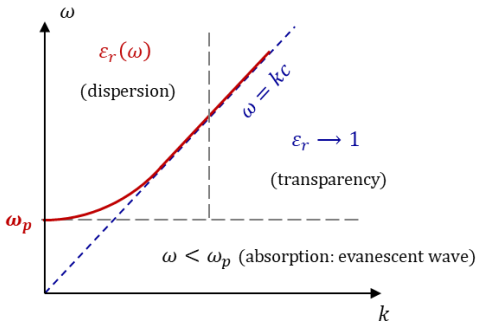

Figure 3. Dispersion relation in the plasma.

The plasma is absorbing (Fig.3) when the microwave frequency is below the plasma frequency:

$$\omega < \omega_p \tag{16}$$

There is a maximum electron density (critical density n_c) from which the plasma is fully reflective:

$$n_c = \frac{m_e\varepsilon_0}{e^2}\omega^2 \tag{17}$$

This property is related to the skin effect as observed in the metals that is expressed in a plasma as:

$$\delta = |k|^{-1} = \frac{c}{\left(\omega_p^2 - \omega^2\right)^{\frac{1}{2}}} \tag{18}$$

Microwave coaxial coupling

When the plasma is created inside a cylinder (Fig.4) above the critical density, it reacts as a conductor (r_p) creating a coaxial waveguide in air with the cavity walls (R) allowing to propagate the microwave in it.

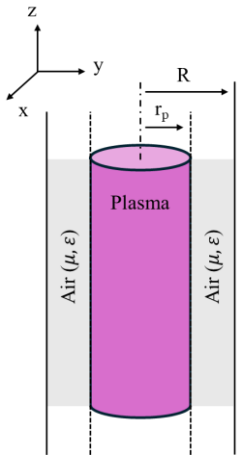

Figure 4. Cross-section of the plasma (coaxial coupling).

In a coaxial waveguide, the TEM mode with $E_z = 0$ and $B_z = 0$ is the dominant mode propagating with no cutoff frequency. Following the dimensions, we can have either a single dominant mode (TEM) or a hybrid mode (TEM+TM/TE). The first secondary mode TE_{11} has a cutoff frequency ω_{11}:

$$\omega_{11} = \frac{2}{\sqrt{\mu\varepsilon}(r_p + R)} \tag{19}$$

Plasma coupling and EEDF

The microwave source is used to transfer the absorbed power P_a from the propagating electric field $E(\omega) = E_0 \cos(\omega t)$ to the electrons [1]:

$$P_a = \frac{n_e e^2}{m_e} \frac{\nu_m}{{\nu_m}^2 + \omega^2} \frac{{E_0}^2}{2} \tag{20}$$

An electron energy loss term by collisions can be considered to solve the Boltzmann equation:

$$\left(\frac{\partial}{\partial t} + \boldsymbol{v}.\boldsymbol{\nabla_r} - \frac{e}{m_e}\boldsymbol{E}.\boldsymbol{\nabla_v}\right) f = \left(\frac{\partial f}{\partial t}\right)_c \tag{21}$$

and compute the Electron Velocity Distribution Function (EVDF) $f(\boldsymbol{r}, \boldsymbol{v}, t)$ [4]. It is recommended to first assume in COMSOL® $f(\boldsymbol{r}, \boldsymbol{v}, t)$ as a Maxwellian distribution, that is a particular solution by considering a uniform, isotropic and stationary solution with no external force and for which the elastic collisions dominate the inelastic collisions. The Maxwell distribution is expressed as:

$$f(\boldsymbol{v}) = n_e \left(\frac{m_e}{2\pi k_B T_e}\right)^{\frac{3}{2}} \exp\left(-\frac{m_e|\boldsymbol{v}|^2}{2k_B T_e}\right) \tag{22}$$

The corresponding Electron Energy Distribution Function (EEDF) as used in COMSOL® is given by:

$$F(\varepsilon) = \frac{2}{\sqrt{\pi}} n_e \sqrt{\varepsilon} \left(\frac{1}{k_B T_e}\right)^{\frac{3}{2}} \exp\left(-\frac{\varepsilon}{k_B T_e}\right) \tag{23}$$

Plasma heating

As the plasma mixture evolves, the thermodynamic properties are computed in space and time for each species from the NASA polynomials [5]. The heat equation is then solved to compute the gas temperature distribution:

$$\left(\rho C_p \frac{\partial}{\partial t} - k\nabla^2\right) T = P_a \tag{24}$$

with boundary conditions to the walls including a heat transfer to the external temperature:

$$-k \frac{\partial T}{\partial n}\Big|_{wall} = h(T_{ext} - T) \tag{25}$$

When the electrons are heated by absorbing the electric field power P_a, they can transmit a part of their kinetic energy by collisions to the heavy particles (neutrals and ions). This reduces their mean energy $\langle\varepsilon\rangle$ leading to an increase of the gas temperature T following the enthalpy balance:

$$\Delta H = C_p \Delta T \tag{26}$$

Plasma production

The plasma production is driven by the particle conservation equation derived from the Boltzmann equation (Zeroth moment):

$$\frac{\partial n}{\partial t} + \boldsymbol{\nabla}.(n\boldsymbol{u}) = G - L \tag{27}$$

where the right-hand side term $G - L$ is the Gains-Losses balance computed from the reaction set and the corresponding reaction rates defined as:

$$R_{eX} = \pm n_e n_X k_{eX} \qquad X = Ar, Ar^+, Ar(4s), Ar(4p) \tag{28}$$

with:

$$k_{eX} = \int_0^{+\infty} \sigma_{eX}(v_e) 4\pi {v_e}^2 f(v_e) v_e dv_e \tag{29}$$

Without applied electric field, the left-hand side term $\boldsymbol{\nabla}.(n\boldsymbol{u})$ is a loss term by diffusion (Fick's law):

$$\boldsymbol{\nabla}.(n\boldsymbol{u}) = -D\nabla^2 n \tag{30}$$

Plasma flow

In a microwave plasma, the charged particle dynamics is mainly driven by the space charge effect and the interaction with the electric field. Thus, we assume that CFD mainly concerns the neutral particle flow following the Navier-Stokes equation. The increase of the gas temperature may induce a gas expansion and thus local accelerations of the flow.

Numerical Model

A microwave plasma is a fully coupled system simulated with the wave propagation (RF module), the formation of the plasma (Plasma module), the heat transfers (Heat transfer module) and the flow regime (CFD module).

RF module

The 'Electromagnetic Waves, Frequency Domain' physics is used with the electric field components solved for 'Three-components vector' in a 'Full field' formulation. The frequency $f = 915$MHz is set in the solver. The 'Wave equation' node computes the wave propagation in all the domains. The 'Perfect Electric Conductor' node is applied to the boundary conditions. The 'Port' node is set for the excitation wave with a 'Rectangular port' and a 'Port input power' defined as P_0/a in W/m where a

is the width of the WR975 waveguide (not represented in 2D). In the mid cross-section plane considered here, the wave satisfies the TEM conditions with $E_z = 0$ and $B_z = 0$. The 'TEM Mode type' is thus selected. The plasma conductivity σ is computed in the plasma domain from the 'Multiphysics Plasma Conductivity Coupling' node through the relationship:

$$\boldsymbol{j} = \sigma \boldsymbol{E} = \frac{n_e e^2}{m_e(i\omega + \nu_m)} \boldsymbol{E} \qquad (31)$$

Plasma module

The 'Plasma' physics is used in the plasma domain with an out-of-plane thickness equal to the Quartz tube diameter. The 'Diffusion Model' is defined as 'Mixture-averaged' to compute automatically the diffusion coefficients for each species. The 'Transport Settings' include 'Calculate thermodynamics properties' based on the NASA polynomials entered for each species, and 'Migration in electric field'. The 'Plasma properties' include 'Use reduced electron transport properties' and 'Include thermal diffusion'. The 'Mean electron energy' is computed in a 'Local energy approximation'. The EEDF is assumed to be a Maxwellian. The volume reactions (Tab.1) for Ar, Ar^+, Ar(4s) and Ar(4p) are defined with the cross-sections and the reaction rates (Tab.2) found in the literature [6] [7].

#	Formula	Type	Δε(eV) [6]
1	e+Ar → e+Ar	Elas.	0
2	e+Ar → e+Ar(4s)	Exc.	11.56
3	e+Ar → e+Ar(4p)	Exc.	13.17
4	e+Ar → 2e+Ar^+	Ion.	15.76
5	e+Ar(4s) → e+Ar(4s)	Elas.	0
6	e+Ar(4s) → e+Ar(4p)	Exc.	1.61
7	e+Ar(4s) → e+Ar	Exc.	-11.56
8	e+Ar(4s) → 2e+Ar^+	Ion.	4.2
9	e+Ar(4p) → e+Ar(4p)	Elas.	0
10	e+Ar(4p) → e+Ar(4s)	Exc.	-1.61
11	e+Ar(4p) → e+Ar	Exc.	-13.17
12	e+Ar(4p) → 2e+Ar+	Ion.	2.59
13	2e+Ar^+ → e+Ar	Att.	-15.76

***Table 1**: List of the volume reactions.*

#	Reaction rate [6]
1	from cross section $\sigma(\varepsilon)$ [7]
2	$5 \times 10^{-15}(T_e)^{0.74} \exp\left(\frac{-11.56}{T_e}\right)$
3	$1.4 \times 10^{-14}(T_e)^{0.71} \exp\left(\frac{-13.17}{T_e}\right)$
4	$2.3 \times 10^{-14}(T_e)^{0.68} \exp\left(\frac{-15.76}{T_e}\right)$
5	from cross section $\sigma(\varepsilon)$ [7]
6	$8.9 \times 10^{-13}(T_e)^{0.51} \exp\left(\frac{11.56 - 13.17}{T_e}\right)$
7	$4.3 \times 10^{-16}(T_e)^{0.74}$
8	$6.8 \times 10^{-15}(T_e)^{0.67} \exp\left(\frac{11.56 - 15.76}{T_e}\right)$
9	from cross section $\sigma(\varepsilon)$ [7]
10	$3 \times 10^{-13}(T_e)^{0.51}$
11	$3.9 \times 10^{-16}(T_e)^{0.71}$
12	$1.8 \times 10^{-13}(T_e)^{0.61} \exp\left(\frac{13.17 - 15.76}{T_e}\right)$
13	$8.75 \times 10^{-39}(T_e)^{-4.5}$

***Table 2**: List of the reaction rates.*

The surface reactions (Tab.3) are applied to the plasma walls. They are defined with a 'Forward sticking coefficient' equal to 1 and no secondary emission.

#	Formula	γ
14	$Ar^+ \rightarrow Ar$	1
15	Ar(4s) → Ar	1
16	Ar(4p) → Ar	1

***Table 3**: List of the surface reactions.*

The 'Species' nodes define the ion and neutral properties found in the literature [5] [8]. The Lennard-Jones (Tab.4) and thermodynamics (Tab.5) properties are important to run a thermal plasma since they contribute to the thermodynamic equilibrium and the gas temperature (T) increase.

Species	σ(Å) [8]	ε/k_B(K) [8]	ΔH(eV) [5]
Ar	3.542	93.3	0
Ar(4s)	3.542	93.3	11.56
Ar(4p)	3.542	93.3	13.17
Ar^+	-	-	15.76

***Table 4**: Lennard-Jones properties.*

NASA polynom. [5]	Ar, Ar(4s), Ar(4p)	Ar^+
T_{lo}	200	298.15
T_{mid}	1000	1000
T_{hi}	6000	6000
$a_{lo,1}$	2.5	2.585
$a_{lo,2}$	0	-1.27111E-3
$a_{lo,3}$	0	5.12646E-6
$a_{lo,4}$	0	-5.84034E-9
$a_{lo,5}$	0	2.13932E-12
$a_{lo,6}$	-7.4537E2	1.82879E5
$a_{lo,7}$	4.37967	5.48413
$a_{hi,1}$	2.5	2.88112
$a_{hi,2}$	0	-1.61448E-4
$a_{hi,3}$	0	1.88409E-8
$a_{hi,4}$	0	1.05317E-12
$a_{hi,5}$	0	-2.99903E-16
$a_{hi,6}$	-7.4537E2	1.82698E5
$a_{hi,7}$	4.37967	3.47047

***Table 5**: NASA polynomial coefficients.*

The 'Initial values' node is set with values by default for the 'Initial mean electron energy' and 'Electric potential', but with a variable input parameter n_{e0} for the 'Initial electron density'. This latter must be tuned manually following the operating conditions to help the model to converge. The 'Wall' and 'Ground' nodes are applied to the plasma walls. The 'Zero Charge' node is applied to the top and bottom boundaries. The 'Insulation' node is applied to the top boundary. The 'Electron Outlet' is applied to the bottom boundary.

Heat transfer module

The 'Heat transfers' physics is used in the plasma and Quartz tube domains with a thickness equal to the Quartz tube diameter. The plasma domain is defined in the 'Fluid' node. The 'Absolute pressure' is coupled with the 'Laminar flow' physics. The 'Heat convection' is coupled with the 'Velocity field'. The 'Thermal conductivity', 'Mean molar mass' and 'Heat capacity at constant pressure' are coupled with the 'Plasma' physics. The 'Initial values 1' are defined with a variable input parameter T_0 for the 'Initial temperature'. The Quartz tube domain is defined in the 'Solid' node from the 'Materials' node (Glass). The 'Initial values 2' are fixed at 300K for the 'Initial temperature'. The 'Heat source' node is applied to the plasma domain with a general 'Heat source for gas' coupled to the 'Plasma' physics. The plasma heating is computed in the plasma domain from the 'Multiphysics Electron Heat Source' node through the relationship:

$$P_a = \frac{1}{2}\Re(\boldsymbol{j}.\boldsymbol{E}^*) \qquad (32)$$

The 'Inflow' node is applied to the top boundary with an upstream temperature defined by the mean domain temperature (aveop1(T)). The 'Outflow' node is applied to the bottom boundary. A 'Heat flux' node is applied to the external walls to stabilize the rise in temperature. A 'Nucleate boiling heat flux' with 'Water' on 'Copper (polished)' has been chosen to ensure an efficient cooling of the walls.

CFD module

The 'Laminar Flow' physics is used in the plasma domain with a reference pressure level p_0. The 'Fluid properties' are coupled with the 'Plasma' physics. The 'Initial values' are set to 0. The 'Wall' node is applied to the plasma walls with 'No slip' conditions. The 'Inlet' node is applied to the top boundary with a 'Fully Developed Flow' and a 'Flow rate' converted in m^3/s from the Standard Liter per Minute units and a time ramp function (Q_{slm}.rm1(t)/60000). The 'Entrance thickness' is equal to the Quartz tube diameter. The 'Outlet' node is applied to the bottom boundary with 'pressure conditions' equal to 0 with 'Normal flow' and 'Suppress backflow' activated.

Study and solver

A 'Frequency-transient' study is used with 'Output times' from 10^{-8}s to 10^{4}s. 'Frequency from solver' is set at 915MHz and 'Laminar Flow' physics is computed in 'Stationary'. The default solver 'Fully Coupled' is applied.

Simulation Results & Discussion

We present first results obtained in a 10kW Argon MW plasma at atmospheric and low pressure. The absolute pressure influences the collision frequency (ν_m) and the electron density (n_e) that play an important role on the relative permittivity $\varepsilon_r(\omega)$ and relative permeability $\mu_r(\omega)$. The simulation results show how the plasma coupling reacts with the microwave and how it changes the topologies of the electric field and plasma density.

Operating conditions

The initial values found for the electron density (n_{e0}) and the gas temperature (T_0) to run the simulations are presented in Tab.6.

10kW	n_{e0} (m^{-3})	T_0 (K)
1000mbar 300slm	1e14	3000
0.001mbar 300slm	1e6	600

***Table 6**: Initial conditions.*

Electron density and electric field

As discussed in the present paper, electron density and electric field are relevant parameters to determine how the plasma is absorbing or not to the microwave. In Fig.5, the TE_{10} mode is absorbed by the plasma and the TEM mode propagates in the coaxial waveguide. The maximum electron density is located at the plasma wall in front of the microwave exposure and follows the expansion of the TEM mode.

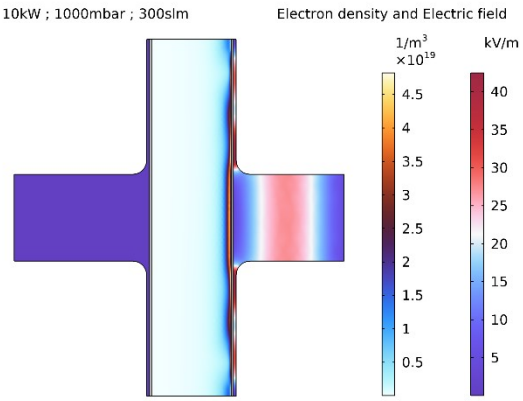

Figure 5. Electron density and electric field at atmospheric pressure.

In Fig.6, the radial profiles at atmospheric pressure are measured in the plasma at y=0mm. The electric field is radially absorbed, and the electron density reacts with a maximum occurring near the exposed plasma wall. At low pressure (Fig.7), the plasma density is too weak to absorb the microwave and the TE_{10} mode propagates like in a transparent material.

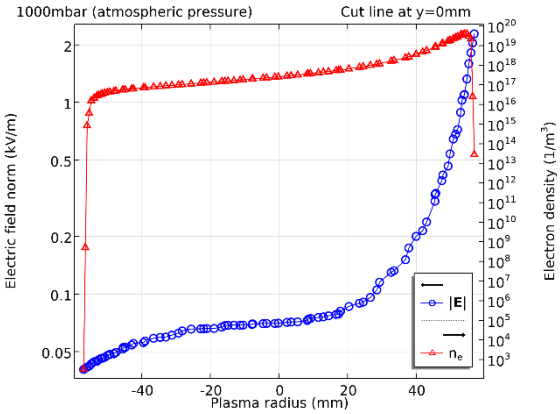

Figure 6. Electron density and electric field profiles at atmospheric pressure.

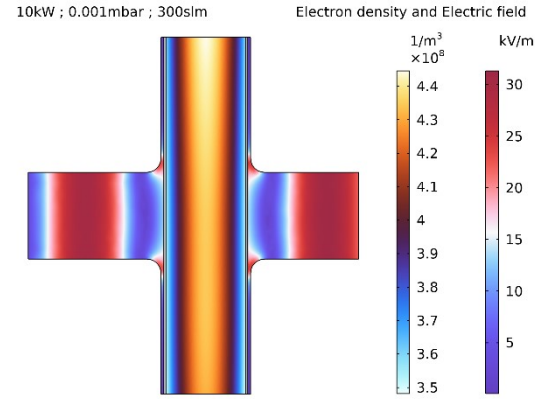

Figure 7. Electron density and electric field at low pressure.

Gas temperature

We have introduced the use of such a MW plasma source to make the thermochemical reactions possible with an increase of the gas temperature. The gas temperature obtained at atmospheric pressure (Fig.8) shows a significant increase up to ~3000K which is in the operating range to ignite a gas decomposition. As observed in the radial profile (Fig.9), the distribution of the gas temperature is asymmetric with a maximum located to the exposed plasma wall.

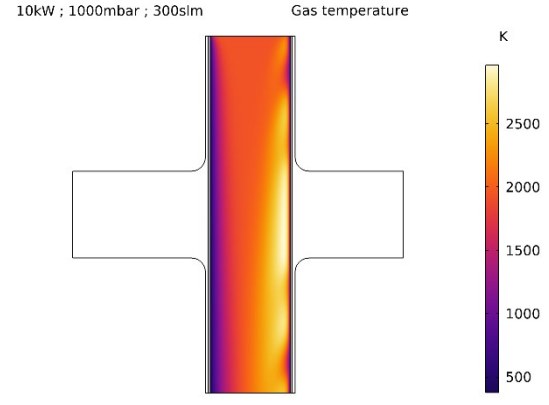

Figure 8. Gas temperature at atmospheric pressure.

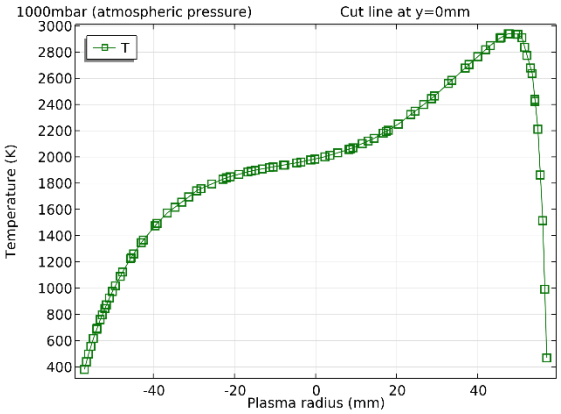

Figure 9. Gas temperature profile at atmospheric pressure.

At low pressure (Fig.10), we observe no change of the gas temperature. Contrary to the thermal plasmas that are ignited from a few mbar with a significant increase of the gas temperature, a low-pressure plasma is classified as a cold plasma with a gas at the external temperature (373K in the present model). In that case, with low collision frequencies, the electron density is too weak to heat the heavy particles significantly.

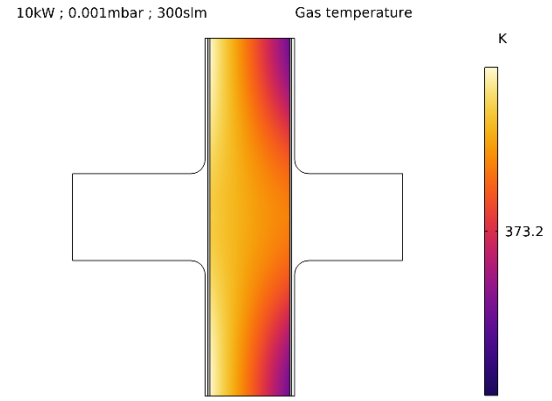

Figure 10. Gas temperature at low pressure.

Conclusions

In the present paper, we have reminded the theoretical aspects occurring in a high-pressure MW plasma. The use of COMSOL Multiphysics® for a plasma simulation at atmospheric pressure is possible thanks to the coupling between the physics of electromagnetics, plasmas, heat transfers and fluid dynamics. As presented, the high-pressure conditions exhibit a strong coupling with the thermodynamic properties that generates an increase in the gas temperature. This behavior is a challenging aspect for plasma modelling at atmospheric pressure. We have also reproduced at atmospheric pressure the skin effect occurring when the plasma is absorbing as expected from the theoretical analysis. The increase in gas temperature, and skin effect are not observed at low pressure making the simulations much easier to be run in a low-pressure regime. In a

future work, the model will be used to establish the scaling laws from the input parameters and the dimensions that are necessary for any improvement. The results will be investigated to identify the stable conditions.

References

[1] M. Moisan and J. Pelletier, Physique des Plasmas Collisionnels - Application aux décharges haute fréquence, EDP Sciences, 2006.

[2] J. M. Rax, Physique des Plasmas, Dunod, 2005.

[3] J. D. Jackson, Electrodynamique Classique, Dunod, 2001.

[4] G. Hagelaar and L. Pitchford, "Solving the Boltzmann Equation to Obtain Electron Transport Coefficients and Rate Coefficients for Fluid Models," *Plasma Sources Science and Technology,* vol. 14, p. 722–733, 2005.

[5] E. Goos, A. Burcat and B. Ruscic, “EXTENDED THIRD MILLENIUM IDEAL GAS AND CONDENSED PHASE THERMOCHEMICAL DATABASE,” [Online]. Available: http://garfield.chem.elte.hu/Burcat/THERM.DAT.

[6] W. Zhang, Recherche numérique et expérimentale sur les propriétés de décharge et les caractéristiques de propagation électromagnétique dans les torches à plasma micro-ondes, Toulouse INP, 2019.

[7] LXCaT, "data type," 2024. [Online]. Available: https://nl.lxcat.net/data/set_type.php.

[8] M. J. Kushner, "Mark Kushner Group - University of Michigan," 2022. [Online]. Available: https://cpseg.eecs.umich.edu/data.html.

Acknowledgements

The author gratefully acknowledges the COMSOL Technical Support team for their help and advises.